International Journal of Engineering Sciences & Research Technology

(A Peer Reviewed Online Journal)
Impact Factor: 5.164

IJESRT

Website: www.ijesrt.com Mail: editor@ijesrt.com

Correspondence Address: 116, Sukhdev Nagar Ext-1, Airport Road, Indore – 452005, Madhya Pradesh, INDIA

RESEARCHERID
THOMSON REUTERS

[Tang* *et al.*, 7(10): October, 2018]
IC™ Value: 3.00

ISSN: 2277-9655
Impact Factor: 5.164
CODEN: IJESS7

IJESRT

INTERNATIONAL JOURNAL OF ENGINEERING SCIENCES & RESEARCH TECHNOLOGY

A METHOD OF SKELETAL FINGER MODEL GENERATION CONSIDERING PHALANGE LENGTH AND JOINT ROTATION AXIS OF INDIVIDUALS

Rong Tang [*1,3], Kazutaka Mitobe[2], Masachika Saito[2] and Noboru Yoshimura[3]
[*1] Graduate School of Engineering and Resource Science, Akita University
[2]Graduate School of Engineering Science, Akita University
[3]Tohoku University of Community Service and Science

DOI: 10.5281/zenodo.1450357

ABSTRACT

Anthropomorphic robot hands are increasingly being utilized to replace the human hand in remote operations or in dangerous places. For most robot hands the skeletal finger models have rotation axes for distal interphalangeal (DIP) joint and proximal interphalangeal (PIP) joint that are usually orthogonal to the finger bones. However, different people may have a different joint rotation axis. Therefore, the aim of this study is to construct a generation method for a finger skeleton model that considers the joint rotation center and axis of individuals, which can significantly influence the accuracy of a finger endpoint when controlling robot hands. This paper introduces generation methods for rotation axis and phalange length from the motion capture data of individuals. Furthermore, we compared the fingertip position generated by the proposed skeletal finger model to a finger model with rotation axes orthogonal to the finger bone. The result was a mean (standard deviation) distance between the fingertip and to all target positions of 2.6 mm (0.9 mm). Compared to a finger model with rotation axes orthogonal to the finger bone, the mean error of the finger model generated by the proposed skeletal finger model was reduced by 45%, and the standard deviation of a finger model generated by the proposed skeletal finger model was reduced by 47%. Additionally, the model generated by the new method had better accuracy and reproduced a more realistic finger motion.

KEYWORDS: motion capture, finger, rotation axis, skeletal finger models, dexterous operation.

1. INTRODUCTION

Anthropologic robot hands have been developed to replace humans hands, such as for tool-manipulation or hazardous material removal, and for dangerous situations [1], [2], [3]. To control anthropologic robot hands, it is necessary to control the angle of each joint, which is very difficult to input manually. Thus, master-slave robot control systems have been developed that utilize motion capture [4], [5]. With a skeletal finger model (link model) and motion capture data, it is possible to control robot hands with motion patterns that are recognized from the contact surface of a skeletal finger model and the target object [4]. Human finger joints are a type of rolling contact joint, and bones are in contact with each other as they roll around. The center of rotation (COR) and axis of rotation (AOR) will shift with changes in joint angles. Therefore, by utilizing a skeletal finger model, we calculated an approximation of COR and AOR in order to control the robot hand. With a skeletal finger model, it is possible to control the posture of the robot hand, and the positional relationship between the finger and target object can be adjusted through optimization methods [5]. However, current techniques can only imitate a grasping motion, and there is no current solution for dexterous motions, such as unbuttoning a shirt or tying shoe laces. There are two possible reasons for this challenge. First, because of high costs, robot hands are standardized with the same finger bone length (segment length) and AOR, which is usually different in mechanical construction from that of the finger operator. Second, there is no established measurement and estimation method for AOR that applies to skeletal finger motion matching the finger of an operator.

In this paper, in order to solve the second problem, we propose a method for measuring and estimating the rotation center and rotation axis vector of the finger joint, which is necessary to design a skeletal finger model and to naturally and realistically reproduce the motion of the operator's finger. In order to evaluate the robustness of our method, we evaluated the estimated AOR determined by our method, and the trajectory and accuracy of fingertip position estimated by the hand skeleton model.

ISSN: 2277-9655
Impact Factor: 5.164
CODEN: IJESS7

Previous research indicates that with an optical motion capture system constructed by cameras and markers, it is possible to calculate the COR of a finger joint by using a least square optimization method [6]. Gamage et al. investigated an AOR estimation method utilizing the least square optimization method for the knee joint and evaluated effectiveness thru simulations [7]. In addition, with the calculation method proposed by Gamage et al, Cerveri et al. presented a calculation method for the COR and AOR of fingers [8]. However, researchers mentioned that using optical motion capture devices incurs occlusion problems when markers enter camera blind spots, which leads to data loss and failures in robot control. To address this issue, we used magnetic motion capture devices that employ electromagnetic waves that pass through hand, thus eliminating such occlusion problems. In our past studies, we analyzed the dexterous hand motions of surgeons and professional piano artists utilizing such a method [9], [10], [11], [12]. In this paper, we will introduce our AOR estimation and evaluation method with magnetic motion capture, including motion for AOR estimation, an evaluation method for fingertip position, and discuss key points regarding the measurement technology that we have developed.

2. MEASUREMENT SYSTEM

A block diagram of the experiment system is shown in Figure 1. Figure 1 (a) shows a block diagram of the measurement system. Our system consists of a PC, Polhemus™ Liberty system, one transmitter, and five receivers. Four receivers are placed on each finger segment and the dorsum of a hand, and one receiver is placed on a stylus. The receivers measure position (x, y, z) and posture (yaw, pitch, roll) relative to the transmitter, with a resolution of 0.0038 mm for position and 0.0012 degrees for posture. Four receivers were placed on a hand, and one on a stylus. The stylus is a device for measuring position and details including calibration methods, which have been introduced in previous research [13]. The mean and standard deviation distance from the position measured by the stylus and true value are 0.5 mm and 0.3 mm, respectively. The stylus is used to measure the target position on the edge of chemical wood, which is used in the evaluation. The size of the chemical wood is L 140 mm ×W 100 mm ×L 50 mm. Figure 1(b) shows an image of the experimental setup, and subjects participating in the experiment are sitting in front of a desk, which is covered with an acryl board. To fit the shape of the finger segments, the receivers placed on the hand were all processed into a teardrop shape. Toupee tape was used between the finger segments and receivers, and kinesiology tape was used to wrap the receivers onto the finger segments and nails. The measurement program was developed with Vizard 4.0 (WorldViz), a Python-based development platform.

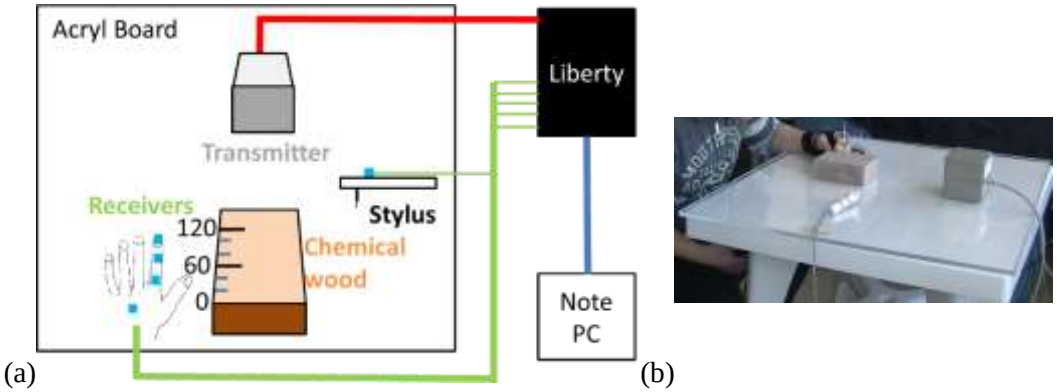

Figure 1. Block diagram of measurement system and photo of experimental setup.

3. METHOD FOR CONSTRUCTING SKELETAL FINGER MODEL AND JOINT ANGLE CALCULATION

An overview of the method for constructing the hand model is shown in Figure 2. There are three main steps for construction of a finger model that accounts for the joint rotation axis of individuals: motion measurement, estimation of joint rotation center and axes, and construction of a finger model. The details are as follows.

- **Motion measurement of finger**

There are two groups of data. One is the hand motion data, and the other are measurements with a stylus at a reference posture. The hand motion used in constructing the finger model is the motion of grasping a circular cylinder, which has been used in previous research for building a skeletal hand model of the human hand [14]. The reference posture is a stretched posture, which is used for defining the Euler angle of the finger segments. At

ISSN: 2277-9655
Impact Factor: 5.164
CODEN: IJESS7

the reference posture, we measure both the data of the receivers placed on hand, and also from the stylus to measure the middle point of the DIP and PIP joint to create the sagittal planes of the fingers. We have described details for creating the sagittal plane of fingers in previous research [13]. In order to evaluate the fingertip when reaching the target position, we also measured the middle point of the distal edge of the finger nail. Because the palm side of the finger deforms when touching a target, we defined the middle point of the distal edge of the finger nail as the fingertip (end point) position of the skeletal finger model.

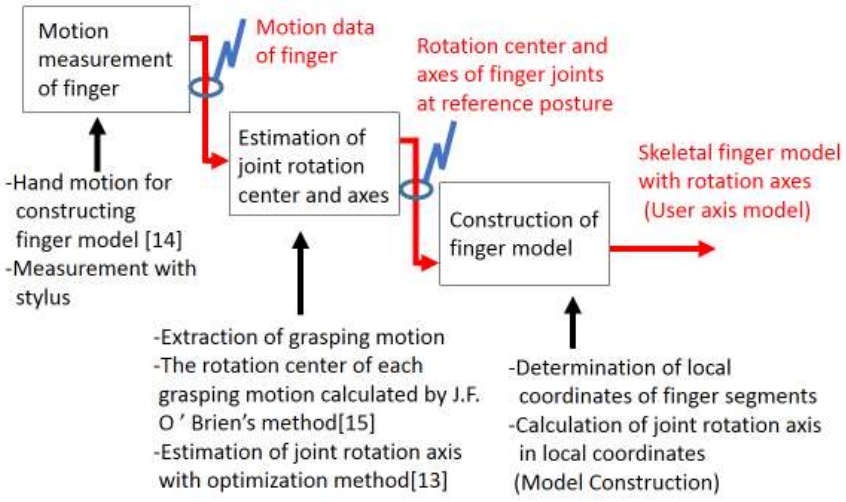

Figure 2. Overview of method for constructing a skeletal finger model.

- **Estimation of joint rotation center and axes**

The estimation method consists of several steps: extraction of the grasping motion, estimation of joint rotation center, and estimation of joint rotation axis. Figure 3 shows a sample of data extracted from a series of grasping motions. When capturing a series for grasping motion, there is always a short period of time for just holding the cylinder or stretching, which the motion data is almost static. Accuracy drops significantly if this kind of data were to be included in the estimation processing for COR and AOR. Furthermore, a grasping motion is the combined movement of the Distal Interphalangeal (DIP) Joint, Proximal Interphalangeal (PIP) Joint and Metacarpophalangeal (MP) Joint, and the dynamic and static period of each joint are slightly different. Therefore, it is impossible to mark the start and end time manually, and it is necessary to have a method for extracting the grasping motion of each finger joint. Thus, we calculated the angle of a joint and angular velocity, and the period $\Delta \boldsymbol{t_i}$ ($i \in \{1, 2, \ldots, 9, 10\}$) of the grasping motion which could be calculated from angular velocity. The calculation method for AOR is as follows:

$$\boldsymbol{J(a)} = \sum_{i=1}^{10} |\boldsymbol{a} \times (\boldsymbol{c}_i - \boldsymbol{e})|^2 \quad (1)$$

Where $\boldsymbol{c}_i$ is the COR of the *i* th grasping motion, $\boldsymbol{a}$ is AOR, and $\boldsymbol{e}$ is one point on the AOR. In this paper, $\boldsymbol{e}$ is the average point of $\boldsymbol{c}_i$, and $\boldsymbol{c}_i$ is calculated from the data at $\Delta \boldsymbol{t_i}$. The calculation method of $\boldsymbol{c}_i$ was developed by J. F. O'Brien, which is used in the COR of limbs [15]. The COR for constructing the skeletal finger model is the intersection of AOR and the sagittal plane, which is the same as in our previous research [13].

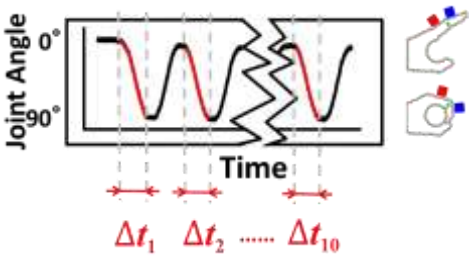

Figure 3. A sample of data extracted from a grasping motion series.

ISSN: 2277-9655
Impact Factor: 5.164
CODEN: IJESS7

- **Construction of skeletal finger model**

We used AOR $\boldsymbol{a}$ and COR to determine the local coordinates. Figure 4 shows the anatomical details and local coordinate system of a skeletal finger model. The gray boxes represent receivers R_i ($i \in \{1, 2, \ldots, 4\}$), and yellow lines represent the finger bones used in the calculations. The blue, green, and red arrows represent the local coordinates of each segment. The origin of the local coordinates are at the end of the distal side. The X axes of the local coordinates are in the same direction as the finger bones, which are calculated by the COR of a joint. Therefore, the Z and Y axes are calculated by

$$\boldsymbol{z} = \boldsymbol{x} \times \boldsymbol{a} \quad (2)$$

$$\boldsymbol{y} = \boldsymbol{z} \times \boldsymbol{x} \quad (3)$$

Where $\boldsymbol{x}$, $\boldsymbol{y}$, $\boldsymbol{z}$ represents each axis of the local coordinates of each finger joint. The skeletal finger models in previous research (orthogonal axis model) use the $\boldsymbol{y}$ axis of local coordinates as the rotation axis of a finger joint [4], [7], [8], where the AORs are orthogonal to the finger bones. Figure 5 shows the skeletal finger model. Figure 5 (a) shows the orthogonal axis model, which used the Y axis of a local coordinate as AOR. Figure 5 (b) shows the proposed user axis model, which consists of the rotation of axis for individuals (user axis model) and the vector of AOR is in purple. Both skeletal finger models consist of finger bones that are represented as a yellow line, and COR is represented as black dots. For the same individual, both models use the same segmental length and COR. With the angle of each joint, position of MP joint, and posture of the dorsum, both skeletal finger models are capable of reacting to a hand motion.

- **Calculation method of joint angle**

Because a small difference in joint angle on a MP joint leads to a significant shifting of fingertip position, the determination of joint angle is important. However, even if AOR $\boldsymbol{a}$ is calculated from motion data, the rotation of the receivers may not be about $\boldsymbol{a}$. Therefore, we proposed a calculation method for joint angle as shown in Figure 6. The gray boxes represent receivers, and the gray circle represent the rotation trajectory of a receiver. $\boldsymbol{r}$ represents the position of a receiver before rotation and $\boldsymbol{r}'$ represent the position after rotation. The purple arrow represents AOR $\boldsymbol{a}$, which is the normal vector of plane S. The blue circle represents the projection of the rotation trajectory of a receiver on plane S, and $\boldsymbol{r}_p$ and $\boldsymbol{r}_p{}'$ represent the projection of $\boldsymbol{r}$ and $\boldsymbol{r}'$. As shown in Figure 6, θ could be calculated from the joint center $\boldsymbol{j}$, $\boldsymbol{r}_p$ and $\boldsymbol{r}_p{}'$.

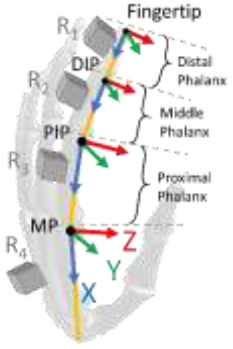

Figure 4. Anatomical detail and local coordinate system of a skeletal finger model.

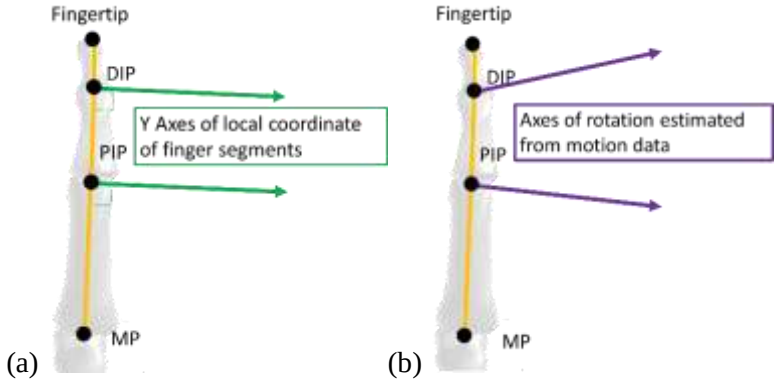

Figure 5. AOR in orthogonal axis model and user axis model.

ISSN: 2277-9655
Impact Factor: 5.164
CODEN: IJESS7

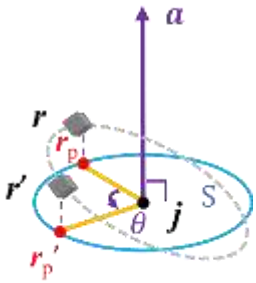

Figure 6. Calculation method for rotation angle around axis with motion data from a receiver.

4. EXPERIMENT AND EVALUATION METHODS

We measured the grasping motion with the left hand to estimate COR and AOR. In total, five people participated in our experiment (about 23 years old on average). In our previous research, we found that receivers will take a tension force from the kinesiology tape when gripping the cylinder. The tension force leads to deviation of posture data, and in the end causes error in the finger joint estimation. In order to solve this problem, instead of using a real cylinder in the experiment, subjects practiced with a cylinder (38.0 mm in diameter, 260.0 mm in height) twenty times in a grasping motion before the experiment. In addition, to unify the measurement time, the tempo of the grasping was kept to within two seconds when grasping.

To evaluate the robustness of the estimation method for AOR and COR, previous research has discussed the standard deviation of the distribution, which means the calculation itself is robust [7], [8]. However, it remains to be seen whether the AOR and COR function correctly in a skeletal finger model. In this paper, in order to evaluate skeletal finger model, we evaluated the accuracy of the fingertip position, which includes the accuracy of AOR, COR and segmental length. With segmental length and COR calculated at a reference position, the fingertip position of the skeletal model during movements were calculated by rotating the distal phalanx about the AOR of a DIP joint, and the position of the DIP joint was calculated from the coordinates of the middle phalanx and joint angle of DIP. Figure 7 shows the positional relationship between the finger and the target used in the evaluation. Figure 7 (a) shows the coordinates of chemical wood and the arrangement of target positions. The origin of the chemical wood is on the 0 mm target, and target positions were arranged on the Z axis. The target positions are 0.7 mm notches with a 20 mm gap between each other, from 0 mm to 120 mm. Figure 7 (b) shows changes in finger angle when reaching the different target positions. Subjects were directed to put the middle point of the thumb fingerprint onto the edge (0 mm position), while the other fingers grip naturally in a way that the subjects felt were comfortable. The change of distance between the index and thumb also reflects a change of joint angle, and the fingertips under a specific distance between the thumb and index were evaluated. The position of targets were estimated by the stylus, and the mean value of five measurements were used as the reference value.

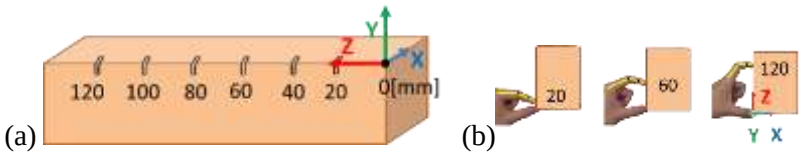

Figure 7. Positional relation between finger and the target in evaluation of AOR.

5. RESULTS

- **Evaluation of AOR for each joint**

To evaluate the AOR of each joint, we calculated the distance between the AOR and the rotation center of ten instances of the grasping motion ($\boldsymbol{c}_i$). Figure 8 shows the distance between the AOR estimated by our method and the rotation centers of each grasping motion calculated by the J. F. O'Brien method. Figure 8 (a) shows the results for DIP and PIP joints, and red boxes represent the results for the DIP joint, and green boxes represent results for the PIP joint. Figure 8 (b) shows the results for the MP joint. As it is shown in Figure 8, the results for the MP joint was a larger distance than for the DIP and PIP joints. For all subjects, the mean (standard deviation) distance between AOR and the rotation center of ten grasping motions for the DIP joint was 0.2 mm (0.1 mm), and 0.3 mm (0.1 mm) for the PIP joint. It is confirmed that the rotation center of each grasping motion was distributed on the AOR, and the calculation for AOR was correct mathematically. We applied the t test to the distance between

ISSN: 2277-9655
Impact Factor: 5.164
CODEN: IJESS7

each joint and there was no significant difference between the DIP group and PIP group ($p > 0.05$). Meanwhile, the MP group showed no significant difference with DIP and PIP. However, we provided the results without considering subject C, where the MP group showed a significant difference for both DIP ($p < 0.01$) and PIP ($p < 0.05$).

- **Evaluation of error in fingertips position during grasping motion**

Figure 9 shows the trajectories of the fingertips calculated with skeletal finger models and the reference position calculated from receivers placed on the distal phalanx. The green dots represent the position calculated from the motion data, and the time between each dot is 0.1 sec. Blue trajectories represent motions to the user axis model, and the red trajectories represent the orthogonal axis model. The vector of the local position of a fingertip at the coordinate of the fingertips were calculated when fingertips were measured with the stylus. With the local position vector, the fingertip positions in a grasping motion were calculated and used as the reference position. As shown in Figure 9 (b) and (c), the user axis model is more consistent with the reference position. In addition, Figure 9 (d) shows that both the user axis and orthogonal models are consistent with the reference position in a Z-X plane. This proves that errors in position increase with the finger bends. Further evaluation was done for the fingertip position when the finger was bent maximally.

Figure 10 shows the error in the fingertip position calculated from the user axis model and the orthogonal axis model with respect to the fingertip position calculated from the receiver placed on the fingertip when a finger was maximally bent. For each subject, we applied a t test between the user axis model and orthogonal axis model. As a result, the error in the user axis model was significantly lower than in the orthogonal axis model ($p < 0.01$) for every subject. Compared with the error for the fingertip position calculated by the orthogonal axis model, the error for the fingertip positions calculated by the user axis model were reduced by 79% for subject B, 49% for subject D and 63% for subject E. In addition, when considering all subjects as one group, the mean (standard deviation) error of fingertips positions calculated by the orthogonal axis model was 5.4 mm (3.4 mm), and was 2.7 mm (1.3 mm) in the user axis model. The t test results also show that the user axis model is significantly different from the orthogonal axis model ($p < 0.01$). Based on the above results, with the user axis model, the mean error for fingertip position was reduced by 50%, and the standard deviation was reduced by 62%. By applying a two-factor factorial ANOVA, the model factor and subject factor were interactive with each other ($p < 0.05$), and as such the results were discarded. However, there is a tendency that subject factor may have caused the differences in the results ($p < 0.05$).

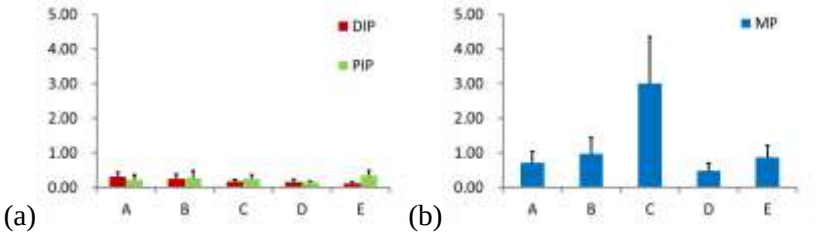

Figure 8. Distance between AOR estimated by our method and the rotation centers for each grasping motion.

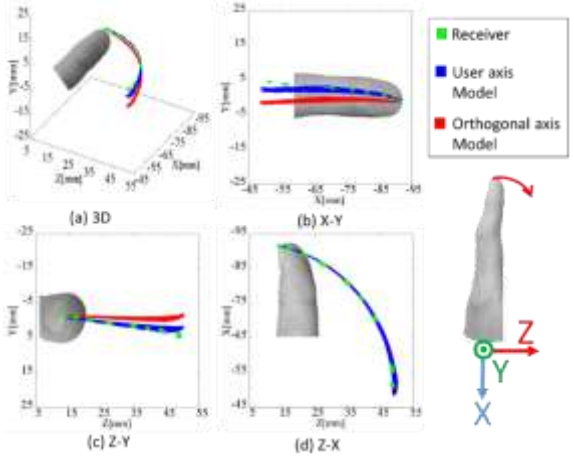

Figure 9. Trajectories of the fingertips calculated with skeletal finger models and the position calculated from a receiver placed on the fingertip.

ISSN: 2277-9655
Impact Factor: 5.164
CODEN: IJESS7

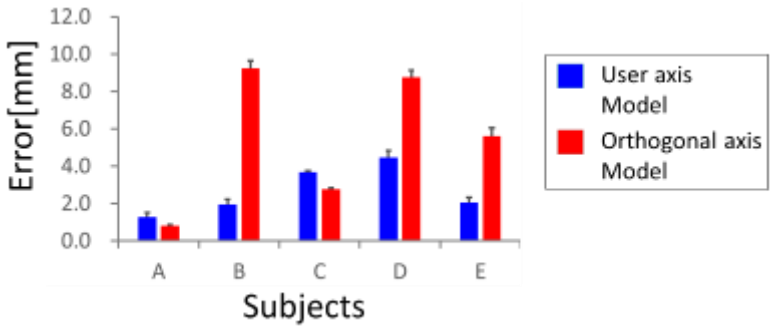

Figure 10. Error of the fingertip position calculated from user axis model and orthogonal axis model with respect to the fingertip reference position (n=10).

- **Evaluation of error for the fingertip position when reaching the target**

Figure 11 shows the distribution of error for the fingertip position calculated with a user axis model and an orthogonal axis model and the fingertip position calculated from the receiver placed on a fingertip with respect to the target position when reaching the target. The target position was represented by a notch on the chemical wood. The triangle represents the position calculated from the receiver placed on the distal phalanx, the circle represents the fingertip position estimated by the user axis model, and square represents the fingertip position estimated by the orthogonal axis model. The color of the marks represents which target the index finger reached, which is green at 20 mm and black at 120 mm. For both skeletal finger models, the lighter the color, the smaller the distance between the fingertips of the thumb and index finger. This shows that to a target position from 20 mm to 80 mm, the error in the end points were gathered, while at over 100 mm the errors shifted towards a plus position.

Figure 12 shows the mean and standard deviation of error of the fingertip position calculated with the user axis model and the orthogonal axis model and the fingertip position calculated from the receiver placed on a fingertip with respect to the target position when reaching the target (n=5). Green boxes represent the error of the fingertip positions calculated from the data of the receiver attached to the distal phalanx, the blue boxes represent the user axis model and the red boxes represent the orthogonal axis model. The mean (standard deviation) error of fingertip positions calculated with the user axis model to all target positions was 2.6 mm (0.9 mm), while the orthogonal axis model was 4.7 mm (1.7 mm). Furthermore, the two-factor factorial ANOVA shows that there was no interaction with the error and the target position ($p > 0.05$), and there was a significant difference between the user axis model and orthogonal axis model. From the discussion above, using user axis model resulted in a mean error of fingertip position that was reduced by 45%, and the standard deviation was reduced by 47% compared to the orthogonal axis model.

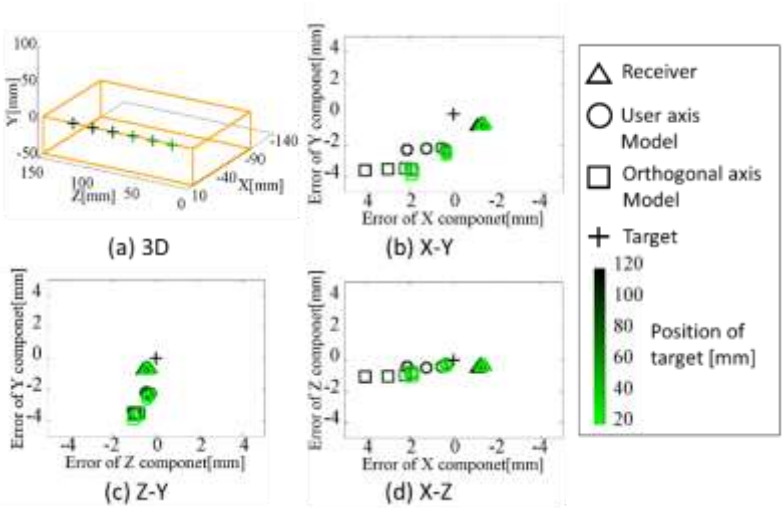

Figure 11. Distribution of error of fingertip position calculated with user axis model and the orthogonal axis model and the fingertip position calculated from the receiver placed on the fingertip with respect to the target position when reaching the target.

ISSN: 2277-9655
Impact Factor: 5.164
CODEN: IJESS7

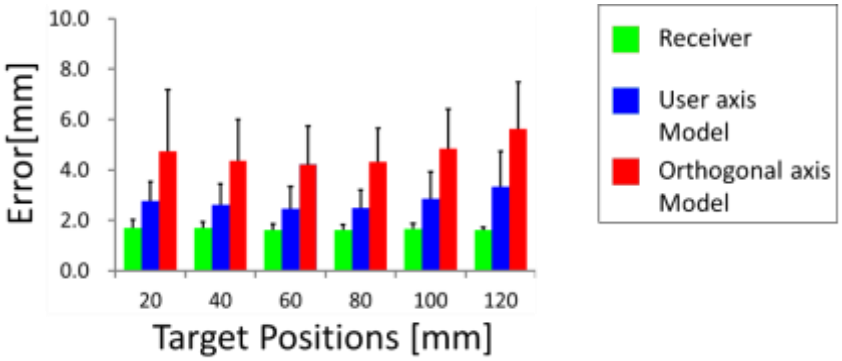

Figure 12. Mean and standard deviation of error of the fingertip position calculated with the user axis model and the orthogonal axis model and the fingertip position calculated from the receiver placed on a fingertip with respect to the target position when reaching the target (n=5).

6. DISCUSSION

The distance between AOR and the rotation center of ten grasping motions of the MP joint is greater than DIP and PIP as shown in Figure 8. Although the grasping motion with four fingers that are close to each other seems to be around one axis of motion for the MP joint, the results confirmed that there is also adduction rotation in the MP joint during grasping.

The errors for fingertip position calculated with the user axis model and orthogonal axis model are small while at a stretched posture in the X-Y plane and Z-Y plane as shown in Figure 9. This is because both the skeletal finger model calculate fingertip position by inputting joint angle to a model at the default posture, which is a stretched posture. Meanwhile, however, the error in AOR leads to a significant error for fingertip position when the finger is maximally bent. The errors for the fingertips can be reduced by using the user axis model as shown in Figure 10. Therefore, accuracy can be improved by applying a user axis model to robot hand design and control systems.

In Figure 11, the distribution of error in the reference position was gathered at all targets, which means the accuracy of the fingertip reference position calculated from a receiver is not dependent on joint angles that change with the position of a target. The results indicate that errors in user axis model are closer to the reference position than from an orthogonal axis model, and the fingertip position calculated with a user axis model has a higher accuracy. Furthermore, when the distance between the thumb tip and index fingertip is above 100 mm, the fingertip positions calculated with the skeletal models shift towards the plus direction of the X axis of coordinates for the chemical wood. In this paper, the middle, ring and pinky finger formed a gripped form while the index finger reached for the targets. As such, the skin around the MP joint of the index finger was pulled by the middle finger, which may have caused the shifting towards the plus direction of the X axis of the coordinates for the chemical wood.

The differences between the user axis model and orthogonal axis model were only in terms of the axis, and both model have the same segmental length, and error for fingertip positions caused by differences in AOR. Using the user axis model reduced the error of fingertip position by 45%. In other words, adjusting the AOR of a robot hand provided a more realistic and precise motion for the robot hand.

7. CONCLUSION

This paper constructed a skeletal finger model to reproduce realistic motions by utilizing a high position-and-posture resolution magnetic motion capture system, model construction, and a joint angle calculation method. In addition, with the skeletal finger model constructed by our method, the calculated fingertip positions were compared with reference positions measured by a stylus. The data from five subjects was used to evaluate and validate our method. The mean distance between AOR estimated by our method and the rotation centers of ten grasping motions calculated by the J. F. O'Brien method indicated that our calculation of AOR were correct. To evaluate the kinematic robustness of AOR and COR, we built skeletal finger models with AOR, and reproduced fingertip positions during a grasping motion. Comparing these results with the fingertips position estimated by motion capture receivers placed on the fingertip confirmed that our skeletal finger model realistically generated

ISSN: 2277-9655
Impact Factor: 5.164
CODEN: IJESS7

the trajectory of the fingertips during the grasping motion. Last, we evaluated errors in fingertip positions estimated by the skeletal finger models to all targets as measured by a stylus. The mean (standard deviation) error of orthogonal axis models used in other research was 4.7 mm (1.7 mm). Compared to the orthogonal axis model, by applying the AOR calculated by our method, the estimation accuracy of the user axis model provided an improvement of 2.6 mm (0.9 mm), which means the error in fingertip position was reduced by 45%. Thus, the proposed AOR calculation method improves the end-point accuracy of a robot hand by adjusting AOR.

This improvement is a result of considered the MP joint as hinge joint in our method, as grasping a cylinder with four fingers close to each other results in the DIP, PIP and MP joint acting as one-axis movement. However, the distance between the AOR and the rotation center for ten repetitions of the grasping motion were bigger than for the DIP and PIP joint, which influences the accuracy of the MP joint position. Although this did not lead to a significant error, a proper estimation method that considers the MP joint as a two-axis or as a ball joint may lead to better position accuracy for the fingertips. Our future research will aim at constructing a skeletal finger model that considers MP as a two-axis joint, which is also necessary for multi-axis joints such as the Carpometacarpal (CM) joint of the thumb.

REFERENCES

[1] S.C. Jacobasen, E.K. Iversen, D.F. Knutti, R.T. Johnson, K. B. Biggers,: Design of the Utah/M.I.T. dexterous hand; *in Proc. IEEE Int. Conf. Robotics and Automation*, pp.1520-1532, (1986).
[2] L.R. Lin, H.P. Huang,: Mechanism Design of A New Multifingered Robot Hand; *in Proc. IEEE Int. Conf. Robotics and Automation*, pp.1471-1476, (1996).
[3] B. M. Jau,: Dexterous telemanipulation with four fingered hand system, *in Proc. IEEE Int. Conf. Robotics and Automation*, pp.338–343, (1995).
[4] F. Cordella, L. Zollo, E. Guglielmelli, B. Siciliano.: A bio-inspired grasp optimization algorithm for an anthropomorphic robotic hand; Int J Interact Des Manuf Vol.6, pp.113-122,(2012).
[5] F. Rotation centerdella, L. Zollo, E. Guglielmelli, B. Sicilinao, et al: A bio-inspired grasp optimization algorithm for an anthropomorphic robotic hand; *International journal of Interact Design and Manufacturing*, Vol.6, No.2, pp.113-122 (2012).
[6] L.Y. Chang, N.S. Pollard: Constrained Least-Squares Optimization for Robust Estimation of Center of Rotation; *Journal of Biomechanics*, In press, (2006).
[7] S.S.H.U. Gamage, J. Lasenby,: New least squares solutions for estimating the average centre of rotation and the axis of rotation; *Journal of Biomechanics*, Vol.35, Issue 1, pp.87-93, (2002)
[8] P. Cerveri, N. Lopomo., A. Pedotti., G. Ferrigno.: Derivation of centers and axes of rotation for wrist and fingers in a hand kinematic model: robust methods and reliability results; Ann. Biomed. Eng. Vol.33,Issue.3, pp.401-411, (2005).
[9] K. Mitobe, J. Kodama, T. Miura, M. Suzuki, N. Yoshimura,: Development of the learning assist system for dexterous finger movements; *ACM SIGGRAPH ASIA 2010 Posters*, No.30, (2010).
[10] Md. M. Rahman, K. Mitobe, M. Suzuki, N. Yoshimura,: Analysis of Finger Movements of a Pianist Using Magnetic Motion Capture System with Six Dimensional Position Sensors; Virtual Real. Soc. Jp 15, 2, pp.243-250 (2010).
[11] Md. M. Rahman, K. Mitobe, M. Suzuki, N. Yoshimura,: Application of Hand Motion Capture System for Piano Education: Virtual Real. Vol.16, Issue.1, pp.83-92, (2011).
[12] Md. M. Rahman, K. Mitobe, M. Suzuki, C. Takano, N. Yoshimura,: Analysis of dexterous finger movement for piano education using motion capture system : Inter. J. Sci.Technol. Vol.2, Issue.2, pp.22-31,(2011).
[13] R. Tang, M. Saito, K. Mitobe, N. Yoshimura,: Method for simplifying magnetic Hand motion capture: position and posture estimation method for finger segments of index with two receivers; International Journal of engineering sciences & research technology. Vol.9, Issue.7, (2018).
[14] B. Buchholz, T. Armstrong, "A kinematic model of the human hand to evaluate its prehensile capabilities," Journal of Biomechanics, Vol.25, No.2, pp.149-162, 1992.
[15] J.F. O'Brien, R.E. Bodenheimer, G.J. Brostow, J.K. Hodgins :" Automatic joint parameter estimation from magnetic motion capture data" , in: Graphics Interface Conference., pp. 53-60, 2000.

ISSN: 2277-9655
Impact Factor: 5.164
CODEN: IJESS7

CITE AN ARTICLE

Tang , Rong, et al. "A METHOD OF SKELETAL FINGER MODEL GENERATION CONSIDERING PHALANGE LENGTH AND JOINT ROTATION AXIS OF INDIVIDUALS ." *INTERNATIONAL JOURNAL OF ENGINEERING SCIENCES & RESEARCH TECHNOLOGY,* vol. 7, no. 10, pp. 20–29.